A Robust Hybrid Iris Localization Technique

Sheikh Ziauddin
Computer Science and Information Management
Asian Institute of Technology
Email: zia.uddin@ait.ac.th

Matthew N. Dailey
Computer Science and Information Management
Asian Institute of Technology
Email: mdailey@ait.ac.th

***Abstract*—In this paper, a new iris localization method is presented. An iris recognition system acquires a human eye image, segments the iris region from the rest of the image, normalizes this segmented image and encodes features to get a compact iris template. Performance of all subsequent stages in an iris recognition system is highly dependent on correct detection of pupil-iris and iris-sclera boundaries in the eye images. In this paper, we present one such system which finds pupil boundary using image gray levels but uses edge detection and circular Hough transform to locate iris boundary. We introduce a number of optimizations to traditional Hough transform based methods. Experimental evaluation shows that the proposed system is accurate and efficient enough for real life applications.**

***Index Terms*—Biometrics, iris recognition, iris segmentation, iris localization, circular Hough transform**

I. Introduction

Iris recognition is one of the most popular biometric authentication technologies due to its uniqueness, stability, robustness and efficiency. In this paper, we focus on the iris *segmentation* problem, in which we must isolate the annular iris region from the rest of the eye image. Most systems find the circular inner and outer boundaries of the iris (this step is generally called iris *localization*) then mark regions of the iris ring that are not visible due to eyelids and eyelashes.

Iris localization is one of the most critical tasks in iris recognition, since all of the downstream processes strongly depend on successful localization. We propose an iris localization technique that achieves very good localization results and hence can be used to enhance the performance of any iris recognition system.

The best known iris recognition system is the one presented by Daugman [1], [2]. He localizes the iris boundary by performing the optimization

$$\max_{(r,x_0,y_0)} \left| G_\sigma(r) * \frac{\partial}{\partial r} \oint_{C(s;r,x_0,y_0)} \frac{I(x,y)}{2\pi r}\, ds \right|,$$

where r and (x_0, y_0) are candidates for the radius and center of the iris, $G_\sigma(r)$ is the one-dimensional Gaussian with standard deviation σ, $*$ is the convolution operator, $C(s; r, x_0, y_0)$ is the circular closed curve with center (x_0, y_0) and radius r, parameterized by s, and $I(\cdot, \cdot)$ is the input eye image. To avoid occlusions caused by eyelids and eyelashes, ds is restricted to the nearly vertical regions of the circle most likely to be visible in the image. The optimization is performed twice to find the iris and pupil circles.

Another important and popular system is that of Wildes [3]. He uses a technique involving edge detection followed by a circular Hough transform. Much of the subsequent work on iris localization builds on this basic approach. A common variation is the usage of a coarse-to-fine strategy. Huang et al. [4] perform rough iris localization in a downscaled eye image and then use the result to reduce the search space for the iris in the full-sized image. Cui et al. [5] also adopt a coarse-to-fine strategy to localize the iris based on a Haar wavelet decomposition. Lili and Mei [6] use image histogram peaks to find rough iris boundaries then refine the resulting boundary. Liu et al. [7] reduce the number of edge points by eliminating the points that correspond to either too-high or too-low intensity values. They use a modified Hough transform and adopt a "hypothesize and verify" technique to filter out candidate boundary circles.

In this paper, we present an iris localization technique using a combination of image intensity thresholding, edge detection, and the circular Hough transform. We use image intensity thresholding to isolate the high-contrast pupil-iris boundary, whereas we use a combination of edge detection and the circular Hough transform to find the lower-contrast iris-sclera boundary.

To evaluate the proposed iris localization algorithm, we test against two datasets: the University of Bath iris image database [8] and the CASIA iris image database [9]. Our experiments show that the proposed scheme is robust as it achieves very good results for both the datasets, with a localization accuracy of 99.5% and 100% for CASIA and Bath, respectively.

II. Hybrid Iris Localization

In the typical iris image captured under near infrared illumination, the pupil-iris boundary has high contrast and the iris-sclera boundary has lower contrast. See Fig. 1 for examples. This observation motivates the design of our algorithm. We use image intensity thresholding to isolate the pupil region from the rest of the image, then we use a circular Hough transform-based technique to find the iris-sclera boundary. Intensity thresholding is much faster than the Hough transform and yields very good results when an appropriate threshold exists, but the performance of thresholding techniques is severely affected when the objects of interest have overlapping intensity distributions. The Hough transform, on the other hand, performs very well in most cases but is computationally

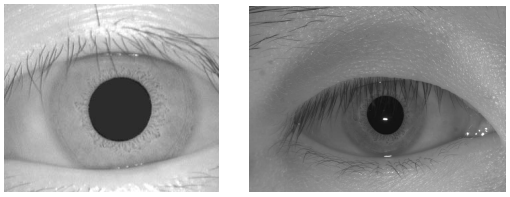

Fig. 1. One iris image each from the CASIA [9] and Bath [8] datasets acquired under near-infrared illumination. The pupil-iris boundary is high contrast, while the iris-sclera boundary is low contrast.

expensive when the parameter space is large. We overcome this limitation of the Hough transform by using the detected pupil's dimensions to crop out regions unlikely to contain the iris-sclera boundary, thus removing unneeded edges from the edge map. Based on the pupil location, we also restrict the Hough search for iris center parameters to a small range. Combined, these enhancements result in efficient iris boundary detection despite the use of the Hough transform. In the following sections, we describe each step of the algorithm in detail.

A. Resizing

In many data sets, the iris images are acquired at quite high resolution. This slows down iris localization unnecessarily. Our first step is thus to resize input images to a reasonable size. The Bath data set images are 1280×960; we downscale them to 25% before proceeding with pupil segmentation. Similarly, the CASIA data set images are 320×280; we downscale them to 50% before proceeding with pupil segmentation. In the rest of this section, mentioned parameter values correspond to the reduced image size.

B. Pupil Segmentation

STEP 1. First we find a threshold suitable for isolating the pupil region from the rest of eye image. The idea is to find an intensity value such that the majority of pupil points and few non-pupil points lie below that value. Although there can be other dark regions, mainly caused by eyelashes or image noise, the pupil is normally the darkest region in an iris image. The dark non-pupil pixels are usually either isolated or form very small clusters. Based on this fact, we first calculate an intensity value i such that the number of points with intensity below i is greater than 0.1% of the total image area. This ensures that the pixels are very likely to include pupil pixels, not only noise and eyelash pixels. We then set the final threshold $T = i + \max(20, 0.4i)$ and apply it to the input image to produce a binary image with the likely candidate pupil area (and noise points) isolated from the background.

STEP 2. The procedure in step 1 is almost always successful in isolating most of the pupil pixels, but some imperfections are common, mainly due to specular reflections from infrared LEDs used to illuminate the iris. In this step, we flood fill the foreground regions from step 1 to eliminate any small holes caused by specular reflection.

STEP 3. Next, we attempt to find a point very likely to be inside the pupil. The idea is to find a large cluster of points and take its center. But in rare cases, the iris image may contain dark, thick eyebrows which form the largest foreground cluster near the top of the binary image. To prevent these regions from being detected as pupil and to speed up the process, we remove foreground pixels from the first 10% rows and the last 10% rows of the image. We do the same for the first 10% and last 10% columns. We can be very confident that the pupil will not lie this close to the image edge in any usable iris image. Then we divide the image in blocks of size equal to the minimum expected radius of pupil circle (15 pixels in downsized images for both the datasets) and count the number of foreground pixels in each block. The block size should be an odd integer so that its center can be located precisely. We take the block which contains the most number of white pixels. The center of this block (b_x, b_y) gives us an initial point very likely to be inside the pupil.

STEP 4. From the point (b_x, b_y), we move in all four directions, one by one, and find the first background pixel in each direction. Let x_l be the first background pixel to the left and x_r be the first background pixel to the right. We set the new x-center to $x_0 = (x_r + x_l)/2$. We then move upward and downward from (x_0, b_y) to find the first background points y_t and y_b. We set the new y-center to $y_0 = (y_b + y_t)/2$ and the new starting point to (x_0, y_0). We repeat the process until the difference between the previous and new values of the center point is not more than one pixel. We let the final estimate of the pupil center (x_p, y_p) to be the result of the final iteration. We then let the final radius estimate be $r_p = (x_r - x_l + y_b - y_t)/4$. Fig. 2 illustrates the results of each step of the procedure.

C. Iris Segmentation

Our iris segmentation technique is based on the well known circular Hough transform method but we make a number of improvements and optimizations that serve both to improve the accuracy of the results and speed up execution. As before, we use downscaled images to reduce the compute time required.

STEP 1. First, we find the relevant region of interest in the input image. Since the pupil center is already known, we crop out regions further than the largest expected iris radius from the pupil center. This radius is dataset dependent; for the CASIA and Bath datasets, we use the values of 65 and 70 pixels, respectively.

STEP 2. Next we smooth the image with a Gaussian filter (standard deviation=2) and obtain the Canny edge map [10] of this blurred image. We use Wildes' [3] idea to find edges only in the vertical direction, as a large number of horizontal edges are caused by eyelids and eyelashes and hence may contribute to incorrect results from the Hough transform.

STEP 3. The result of step 2 normally contains a number of unwanted edges whose removal would enable faster and more accurate iris localization. In this step, we remove as many of these unwanted edges from the edge image as possible. We observe that there are three main factors contributing to false iris circle detection with the Hough transform. First, edges

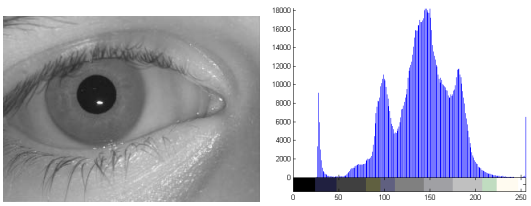

(a) Input eye image (b) Image histogram

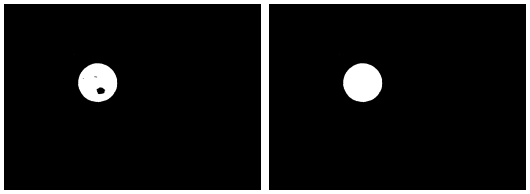

(c) Binary image (d) Binary image after flood-fill

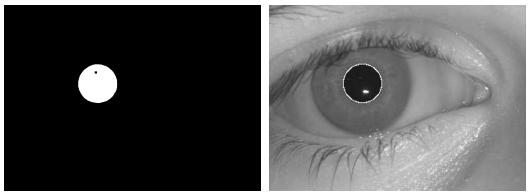

(e) Point found inside pupil (point enlarged for visibility) (f) Detected pupil boundary marked on the image

Fig. 2. Pupil segmentation procedure. Image is from the Bath data set [8].

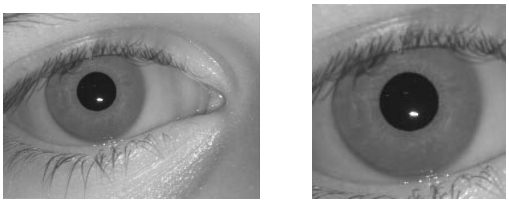

(a) Input eye image (b) Cropped image

(c) Edge image (d) Template to eliminate false edges

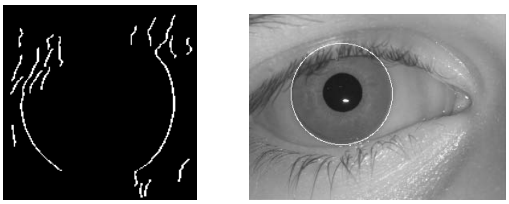

(e) Reduced edge image (f) Detected iris boundary marked on the image

Fig. 3. Iris segmentation procedure illustrated on a Bath data set [8] image.

corresponding to the pupil boundary are present in the edge image. These edges are generally stronger than the iris-sclera boundary edges due to the higher contrast between pupil and iris and thus are sometimes confused with the iris boundary. Second, sometimes furrows close to the pupil boundary cause false detections. When one of the sides of the iris does not generate long enough edges but furrows near the pupil do, the Hough transform may mistakenly connect one true iris side with a false side created by furrows. Finally, some of the longer upper eyelashes can also contribute toward detection of false circles. To mitigate the effect of these factors, we define a binary mask for each image that eliminates many such undesirable points from the edge image. All edge pixels corresponding to the mask in Fig. 3(d) are eliminated from consideration by the Hough transform. The size of the template is not fixed but rather depends on the size of pupil radius r_p in each image. The width of the upper and lower thinner part of the template is $2r_p$, while that of the middle thicker part is $2r_{min}$ where r_{min} is the minimum expected iris radius in the dataset (we use $r_{min} = 40$ for both datasets). The height of middle portion is $2r_p$ and the whole template is centered on the pupil center. In addition to the application of binary mask, we apply two further operations on the resultant edge image. First we apply a simple thresholding to remove the portions of the dark eyelashes which were not removed by the binary mask. Second we retain only those connected foreground components in the edge image having the number of pixels greater than an appropriate threshold value (we use a value of 20 pixels for both datasets). This retains two large arcs corresponding to the left and right iris boundaries and removes many unwanted smaller components.

STEP 4. As a final step, we apply the circular Hough transform to find the circle best fitting the edge image from step 3. To speed up the Hough transform, we restrict the parameter estimates based on the pupil center and radius; although the pupil and iris circles are not necessarily concentric, they are almost always very nearly so. We thus restrict the center coordinates (x_i, y_i) of the iris circle such that $x_p - 5 \leq x_i \leq x_p + 5$ and $y_i = y_p$ where x_p and y_p are center coordinates of the pupil. The intuition behind using tighter restrictions along the vertical axis is that our edge image contains vertical edges, so when we move vertically away from y_p, we are more likely to encounter false edges. Our experimental results show that this assumption is correct. Fig. 3 illustrates the steps of the iris localization procedure.

III. EXPERIMENTAL EVALUATION

A. Iris Dataset

We performed experiments using the University of Bath [8] and CASIA [9] version 1 iris datasets to evaluate the segmentation accuracy of our scheme. Version 1 of the CASIA dataset consists of 7 iris images captured from each of 108 subjects, for a total of 756 images. The free version of the Bath dataset consists of 20 iris images of each eye captured from each of 25 subjects, for a total of 1000 images. We tested our algorithm on the right eye images of all 25 Bath subjects.

TABLE I
IRIS LOCALIZATION RESULTS.

	Bath	CASIA
Accuracy	100%	99.5%
Mean Time	0.42 s	0.24 s

TABLE II
COMPARISON OF IRIS LOCALIZATION RESULTS ON THE BATH DATASET.

	Masek's system	Our system
Accuracy	81%	100%
Mean Time	119 s	0.42 s

TABLE III
COMPARISON OF IRIS LOCALIZATION RESULTS WITH EXISTING SYSTEMS.

Method	Accuracy	Mean Time
Daugman	98.6%	6.56 s
Wildes [3]	99.9%	8.28 s
Wildes [13]	99.5%	1.98 s
Cui	99.3%	0.24 s
Xu	98.4%	-
Chavez	99.9%	0.07 s
Proposed	99.5%	0.24 s

Our algorithm is thus evaluated against a total of 756 CASIA images and 500 Bath images.

B. Segmentation Results

We applied our algorithm to all dataset images and evaluated the accuracy for finding the pupil-iris and iris-sclera boundaries. The source code was written in MATLAB. The experiments were performed in MATLAB 7.0 running on Windows XP 2002 with service pack 2. The PC was an Intel Pentium-4 2.66 GHZ processor with 2.5 GB of DDR-333 RAM. We verified the results manually. Table I summarizes our results.

We should mention here that in version 1 of CASIA, the pupil area of each image was edited manually and replaced with a circular region of constant intensity. Due to this manual editing, CASIA version 1 is not recommended for research anymore [11]. But as most of the previous results have been reported on this dataset, we opted to report results on both the CASIA and Bath datasets. For Bath, we compared the accuracy and speed of our system with the only (to the best of our knowledge) open source iris recognition implementation available, written by Masek and Kovesi [12]. We ran Masek's segmentation algorithm on our resized Bath iris dataset images and compared the results. Table II provides a comparison of our system with Masek's on Bath dataset while Table III provides a comparison of our system with other existing systems on CASIA dataset.

On the Bath dataset, we achieve much improved results compared to Masek's system. On Casia, we achieve results comparable to current state of the art systems both in terms of speed and accuracy. This is one of very few papers reporting specific iris localization results on multiple datasets having quite different characteristics. We apply exactly the same algorithm on both datasets and, with a few exceptions (e.g., the upper and lower bounds on the expected pupil and iris radii), all the system parameters are dataset independent.

IV. CONCLUSIONS

In this paper, we propose and evaluate a scheme for accurately localizing the iris in images acquired for iris recognition systems. As opposed to most existing schemes, which either use image intensity or Hough transform for this purpose, we use a hybrid technique involving a combination of both these methods. In an experiment on Bath and CASIA, we find that the method successfully combines the desirable features of both techniques, resulting in a robust and fast iris localization system.

ACKNOWLEDGEMENTS

We are grateful to Bath University and the Chinese Academy of Sciences Institute of Automation for their iris datasets and to Libor Masek and Peter Kovesi for their Matlab iris recognition source code.

REFERENCES

[1] John Daugman, "High confidence visual recognition of persons by a test of statistical independence," *IEEE Transactions on Pattern Analysis and Machine Intelligence*, vol. 15, no. 11, pp. 1148–1161, 1993.

[2] John Daugman, "The importance of being random: statistical principles of iris recognition," *Pattern Recognition*, vol. 36, no. 2, pp. 279–291, Feb. 2003.

[3] Richard Wildes, "Iris recognition: An emerging biometric technology," *PIEEE*, vol. 85, no. 9, pp. 1348–1363, September 1997.

[4] Y.P. Huang, S.W. Luo, and E.Y. Chen, "An efficient iris recognition system," in *Machine Learning and Cybernetics, 2002. Proceedings. 2002 International Conference on*, 2002, vol. 1.

[5] J. Cui, Y. Wang, T. Tan, L. Ma, and Z. Sun, "A fast and robust iris localization method based on texture segmentation," in *Proceedings of SPIE*, 2004, vol. 5404, pp. 401–408.

[6] P. Lili and X. Mei, "The algorithm of iris image processing," in *Fourth IEEE Workshop on Automatic Identification Technologies*, 2005, pp. 134–138.

[7] X. Liu, KW Bowyer, and PJ Flynn, "Experiments with an Improved Iris Segmentation Algorithm," in *Automatic Identification Advanced Technologies, 2005. Fourth IEEE Workshop on*, 2005, pp. 118–123.

[8] University of Bath, "University of Bath Iris Image Database," 2004, http://www.bath.ac.uk/elec-eng/research/sipg/irisweb/.

[9] "CASIA Iris Image Database," Chinese Academy of Sciences - Institute of Automation (CASIA), 2004, http://www.sinobiometrics.com.

[10] J. Canny, "A computational approach to edge detection," *IEEE Transactions on Pattern Analysis and Machine Intelligence*, vol. 8, no. 6, pp. 679–698, 1986.

[11] P. J. Phillips, K. W. Bowyer, and P. J. Flynn, "Comments on the CASIA version 1.0 iris data set," *IEEE Trans. Pattern Analysis and Machine Intelligence*, vol. 29, no. 10, pp. 1869–1870, Oct. 2007.

[12] Libor Masek and Peter Kovesi, *MATLAB Source Code for a Biometric Identification System Based on Iris Patterns*, The School of Computer Science and Software Engineering, The University of Western Australia, 2003, http://www.csse.uwa.edu.au/~pk/studentprojects/libor/sourcecode.html.

[13] T. A. Camus and Richard Wildes, "Reliable and fast eye finding in close-up images," in *ICPR*, 2002, pp. I: 389–394.